UV Resonance Raman Study of the Spatial Dependence of α-Helix Unfolding[†]

Anatoli Ianoul, Alexander Mikhonin, Igor K. Lednev, and Sanford A. Asher*

Department of Chemistry, University of Pittsburgh, Pittsburgh, Pennsylvania 15260

Received: September 14, 2001; In Final Form: January 7, 2002

We used ultraviolet resonance Raman (UVRR) spectra to examine the spatial dependence and the thermodynamics of α-helix melting of an isotopically labeled α-helical, 21-residue, mainly alanine peptide. The peptide was synthesized with six natural abundance amino acids at the center and mainly perdeuterated residues elsewhere. C_α deuteration of a peptide bond decouples C_α−H bending from N−H bending, which significantly shifts the random coil conformation amide III band; this shift clearly resolves it from the amide III band of the nondeuterated peptide bonds. Analysis of the isotopically spectrally resolved amide III bands from the external and central peptide amide bonds show that the six central amide bonds have a higher α-helix melting temperature (∼32 °C) than that of the exterior amide bonds (∼5 °C).

Introduction

An elucidation of the mechanism of protein folding requires the understanding of the structural and dynamical aspects of α-helix unfolding.[1−4] Previous theoretical examinations of α-helix unfolding predicted that at equilibrium all but the longest α-helices would contain only a single helix sequence and that this helix would unfold from its ends.[5] Recent transient fluorescence probe,[6,7] IR absorption,[4] and UV resonance Raman (UVRR) studies[1,8] have found that the unfolding dynamics occurs on a 200 ns time scale and that the kinetics have the appearance of a two state unfolding mechanism. However, detailed kinetic temperature-dependent measurements indicate that the unfolding does not show a simple two state Arrhenius behavior.[1] This clearly signals that the true mechanism follows an intrinsically complicated energy landscape.

Our recent kinetic UVRR investigations[1,8] have allowed us to examine the dynamics of peptide unfolding by examining the evolution of the UVRR spectra caused by a ns T-jump. The Raman spectra are highly resolved and can be used to quantitatively determine the secondary structure composition. The obvious next step in the study of the helix unfolding process is to understand the spatial dependence of unfolding.

We show here that it is possible to determine the spatial dependence of peptide unfolding through isotopic labeling. Isotopic labeling shifts the vibrational bands such that the conformational evolution of an isotopically labeled region can be resolved from the conformational evolution of an unlabeled region. We, thus, measure the temperature-induced melting of different parts of the α-helix, and find different melting temperatures for the exterior versus the central peptide amide bonds.

Experimental Section

Materials. The deuterated alanine was obtained from Glycopep Chemicals, Inc. The alanine based polypeptide (AP) of composition $A_5(A_3RA)_3A$ and the deuterium labeled peptide

AAAAAAAA-RAAAAR-**AAAA**-R-**AA** (AdP)

where **A** is L-Ala(2,3,3,3-D₄) were synthesized (>95% purity)

at the Pittsburgh Cancer Institute by the solid-phase peptide synthesis method.

Instrumentation. The UV−Raman instrumentation is described in detail elsewhere.[1,8] UVRR spectra were measured using 204 nm excitation obtained by anti-Stokes Raman shifting the third harmonic of an Infinity YAG laser (Coherent Inc.) in H_2. The Raman scattered light was collected in a ∼135° backscattering geometry and dispersed by a Spex double monochromator. An intensified CCD detector (Princeton Instruments Co.) was used for detection. The samples were measured in a temperature-controlled free-surface flow stream.

All spectra were normalized to the ClO_4^- internal standard band at 932 cm⁻¹. The broad 1640 cm⁻¹ H_2O Raman bending band was subtracted using a measured solvent reference spectrum.

The CD spectra were measured by using a Jasco 710 spectropolarimeter.

Results and Discussion

To spectrally spatially resolve the central from the exterior peptide bonds we compared the UVRR of natural abundance AP to the deuterium labeled peptide **AAAAAAAA-**RAAAAR-**AAAA**-R-**AA** (AdP), where **A** is L-Ala(2,3,3,3-D₄). Both peptide termini are fully deuterated, except for the residue nineteen arg group, while the central two arg and the four ala are natural abundance.

UVRR Spectra of AP and AdP. Figure 1 shows 204 nm excited UVRR spectra of AdP and the natural abundance alanine peptide (AP) at low (−0.2 °C) and high (+70 °C) temperatures as well as their temperature difference spectra. AP at 70 °C is essentially pure random coil and shows bands at ∼1660 cm⁻¹, ∼1550 cm⁻¹, ∼1380 cm⁻¹, and ∼1249 cm⁻¹ which are assigned to the amide I, amide II, $C_\alpha H$ bending and amide III vibrations, respectively.[1] We measure an amide III Raman cross section of ∼60 mBarn/(peptide bond·sr).

As shown previously, the temperature-induced spectral differences result from the α-helix→random coil transition combined with a modest temperature dependence for the random coil Raman bands.[1] The AP difference spectrum (Figure 1c) shows a peak at 1234 cm⁻¹ due to the loss of the random coil amide III intensity. The broad peak at ∼1377 cm⁻¹ derives from the loss of the random coil C_α−H bending band. Other
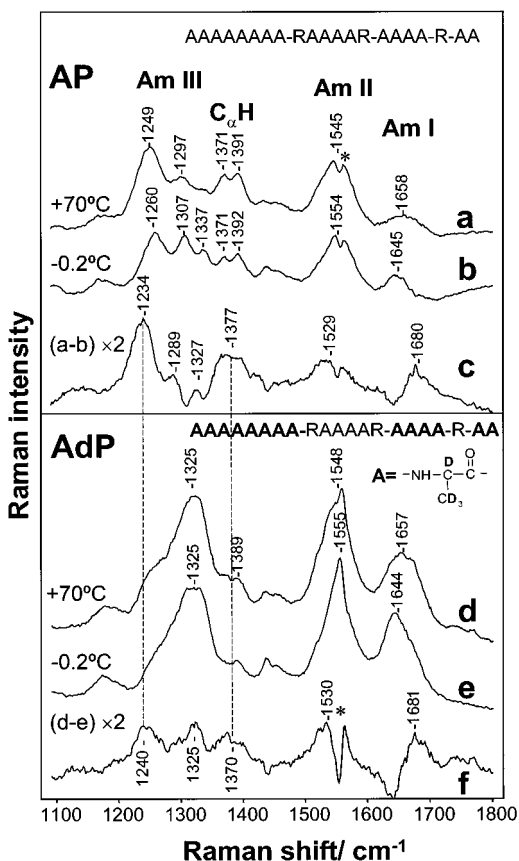
Figure 1. 204 nm excited UV RR spectra of the 21 unit peptide AP (AAAAAAAA-RAAAAR-AAAA-R-AA) (a, b, c) and the deuterated peptide AdP (**AAAAAAAA**-RAAAAR-**AAAA**-R-**AA,** where **A** is L-Ala(2,3,3,3-D₄)) (d, e, f) at −0.2 °C (b, e), +70 °C (a, d) and their difference spectra (c, f). The experimental setup is described in reference 1. The 932 cm⁻¹ band of 0.15 M sodium perchlorate was used as an internal standard, and the peptide concentrations were 0.5 mg/mL. We utilize a spectral accumulation time of 20 min, with a spectral resolution of ~10 cm⁻¹. The star marks a peak assigned to molecular oxygen. Spectra (c) and (f) were multiplied by 2.
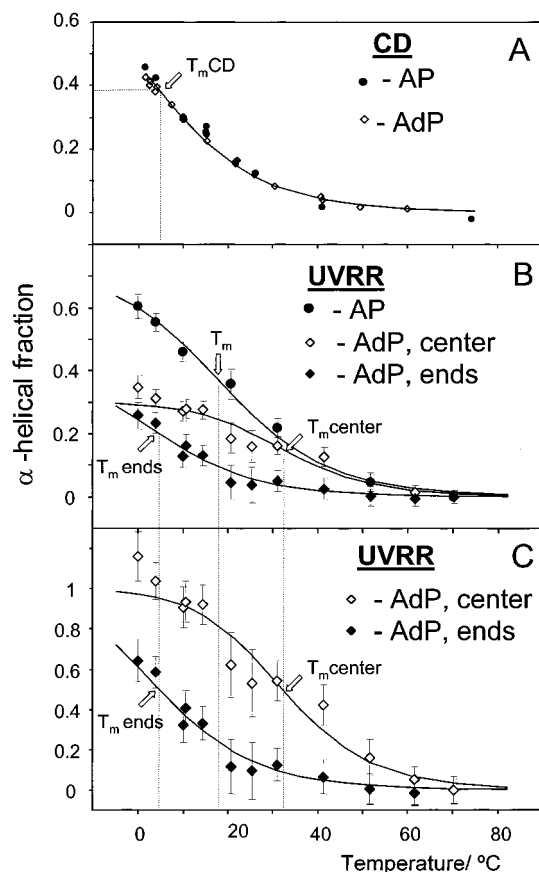

Figure 2. (A) Temperature dependence of the AP and AdP α-helicity as calculated from CD measurements using the method described in ref 1. The CD data were fitted to expressions for the molar ellipticity analogous to eqs 1 and 2 assuming the maximum α-helical fraction 0.78.¹ (B) α-Helical fraction temperature dependence calculated from the UVRR of AP (●), nondeuterated central amide bonds (◇), and deuterated external amide bonds (◆) of AdP. The α-helix composition was ratioed to the total number of AdP peptide bonds (twenty). Solid lines are the best fits obtained using eqs 1 and 2 with the parameters listed in Table 1, assuming the maximum α-helical fractions 0.7 for AP, 0.3 for the central peptide bonds of AdP, and 0.4 for the external peptide bonds of AdP.¹ (C) α-Helical fraction temperature dependence from Figure 2B normalized to the number of peptide bonds of the central and of the external segments that can form an α-helix. Solid lines are the best fits obtained using eqs 1 and 2 with the parameters listed in the Table 1.

difference features also occur, such as the derivative shaped amide I feature, due to the fact that the random coil amide I band occurs at higher frequency than does the α-helix form.

The UVRR spectra of AdP differ from those of AP mainly in an upshift of the C$_\alpha$ deuterated amide III band to ~1325 cm⁻¹.⁹⁻¹³ The deuterated amide III band displays a dramatically increased Raman cross section of ~217 mBarn/(peptide bond· sr). In addition, the C$_\alpha$−H bending band intensity decreases due to deuteration of some of the C$_\alpha$ carbon amide bonds.

Thus, the ~1325 cm⁻¹ band intensity derives mainly from the amide III band from the deuterated amide bonds. The nondeuterated part of AdP shows a spectrum similar to that of AP (Figure 1); the shoulders observed at ~1240 and 1380 cm⁻¹ in the spectrum of AdP derive from the amide III bands of the nondeuterated amide bonds. The remainder of the AdP spectrum is very similar to that of AP.

The AdP difference spectrum shows peaks at 1240, 1325, and 1370 cm⁻¹, in addition to the derivative shaped amide I difference band (Figure 1f). The 1240 and 1370 cm⁻¹ peaks are similar to those in the AP difference spectrum (Figure 1c). They derive from the amide III and C$_\alpha$H bending bands of the increased concentration random coil conformation within the nondeuterated, center of AdP. In contrast, the 1325 cm⁻¹ band, absent in the difference spectrum of AP (Figure 1c), derives mostly from the deuterated part of AdP and is dominated

by the conversion of deuterated amide bonds from the α-helix to the random coil conformation.

The intensity of the 1325 cm⁻¹ deuterated amide III difference spectral peak is determined mainly by the difference in the amide III Raman cross section between the α-helix and the random coil deuterated amide bonds, since there is little change in the amide III frequency between the α-helix and random coil conformations. The temperature dependence of the frequencies appears to be negligible, as is evident from the lack of a derivative feature in the difference spectrum.

The intensities of the 1240 and 1370 cm⁻¹ difference spectral peaks are determined mainly by the increase in the number of random coil amide bonds, since only random coil amide bonds give rise to the peaks at 1235 and 1370 cm⁻¹. Thus, the magnitude of the deuterated and nondeuterated peptide bond temperature difference spectral peaks is proportional to the total number of amide bonds undergoing the conformational transition from α-helix to random coil.

Melting of AP and AdP. Figure 2A shows the calculated α-helical fractions of AP and AdP determined from their

Spatial Dependence of α-Helix Unfolding

J. Phys. Chem. A, Vol. 106, No. 14, 2002 **3623**

TABLE 1: Thermodynamic Parameters[a] for AdP and AP Coil↔Helix Transition

	T_m °C	ΔH kcal/mol$_{peptide}$	ΔS kcal/(mol$_{peptide}$·K)
AP	17±5	−14.8±2	−51±6
AdP, ends	5±5	−14.4±4.1	−51.9±14
AdP, center	32±5	−18.7±5.5	−61.2±18

[a] The thermodynamic parameters are listed with the standard errors (±2σ). We fitted the melting curves of Figure 2 with eqs 1 and 2 using the Levenberg−Marquardt approximation procedure (SPSS software). These equations have three independent parameters, ΔH, ΔS, and the maximum α-helical fraction f_{max} (or fd_{max}). If we determine all three parameters from fitting, without constraints, the errors in determination of those parameters will be much higher than those presented in Table 1. However, we estimated the maximal helical fractions f_{max} and fd_{max} from independent data, as noted above, and used them as fixed parameters in our fitting. This resulted in the smaller standard errors quoted in Table 1. The parameters ΔH and ΔS mutually compensate, which increases their estimated standard errors.

measured CD spectra, according to the method described in ref 1. Figures 2B and 2C show the calculated α-helical fraction of AP and the spatially resolved calculated α-helical fractions of the central six and exterior fourteen amide bonds of AdP determined by analyzing the UVRR spectra as described in the appendix below.

The Figure 2A CD data show the expected identical α-helix melting curves for AdP and AP, which yield $T_m = 5$ °C for the average peptide bond melting temperatures. As previously[1] discussed in detail, we calculate a significantly higher average peptide bond $T_m = 17$ °C from the Figure 2B UV Raman data because the Raman spectra more heavily weight shorter α-helical segments than do the CD spectra.[1,14] This modeling assumes that a total of six penultimate residues will not form an α-helix, since they cannot have both stabilizing α-helix hydrogen bonds. Thus, we expect that a maximum of eight of the thirteen deuterated external peptide bonds can be involved in an α-helix (62% maximum α-helix fraction).

The Figure 2B peptide melting curves are scaled to the total number of amide bonds (twenty), while the Figure 2C melting curves are scaled to show the relative α-helical fraction of the central six residues and the relative α-helical fraction of the exterior eight dueterated residues that can potentially fom an α-helix.

Figures 2B and 2C show significantly different melting curves for the central and exterior AdP peptide bonds. The six central peptide bonds show a complete melting curve with an apparent $T_m = 32$ °C (Figure 2C). The central six peptide bonds are essentially 100% α-helical at 0 °C and have negligible α-helix content at 60 °C.

In contrast, the exterior peptide bonds are ~60% α-helical at 0 °C and are negligibly α-helical by 40 °C. We calculate a $T_m = 5$ °C. Thus, at the average AdP and AP peptide bond melting temperature of $T_m = 17$ °C, where the α-helix conformation involves half (seven) of all of the amide bonds capable of forming an α-helix (fourteen), ~80% of the six central amide bonds (~five) occur in an α-helix. In contrast, only ~20% of the exterior peptide amide bonds (eight) are α-helical (approx. two) as shown in Figure 2C. These results, which demonstrate a decreased T_m for exterior amide bonds, are predicted by theory[5] and are similar to the results of ^{13}C NMR studies of the α-helical peptide acetylW(EAAAR)$_3$A.[15]

We calculated the thermodynamic parameters for the central and exterior peptide bonds (Table 1) from the UVRR melting curves by assuming the simplest two-state model for both internal as well as penultimate amide bonds of AdP:

$$f_\alpha(T) = \frac{f_{max}}{1 + \exp\left(-\dfrac{\Delta H}{RT} + \dfrac{\Delta S}{R}\right)} \tag{1}$$

$$fd_\alpha(T) = \frac{fd_{max}}{1 + \exp\left(-\dfrac{\Delta H_d}{RT} + \dfrac{\Delta S_d}{R}\right)} \tag{2}$$

Here $f_\alpha(T)$ and $fd_\alpha(T)$ are the temperature-dependent fractional α-helix content of the central and exterior peptide bonds, while f_{max} is the maximum α-helix fraction of the six central nondeuterated peptide bonds; fd_{max} is the α-helix fraction of the eight exterior peptide bonds which can occur in an α-helix; and $f_{max} = 6/20 = 0.3$ and $fd_{max} = 8/20 = 0.4$.

Although we see clear differences in T_m, the differences in ΔH and ΔS for the central residues compared to the external residues, are within the error bars of the modeling, due to the limited spectral signal-to-noise ratios. We will revisit this issue in the future when we obtain higher signal-to-noise ratio data from higher concentration peptide samples; we presently have only small amounts of the AdP peptide.

Conclusions

The work here demonstrates that UVRR of a selectively deuterium labeled α-helical peptide allows us to spatially resolve the conformation of individual peptide bonds. We observe significantly higher T_m values for peptide bonds in the center of the peptide compared to the external peptide bonds. We are beginning nsec UV resonance Raman T-jump studies of this peptide to spatially resolve the dynamics of α-helix unfolding.

Appendix

Spectral Analysis. The AP α-helical fraction was calculated from the AP Raman spectra using the temperature-dependent AP α-helix and random coil basis Raman spectra and the procedure of ref 1.

We modeled the AdP UVRR spectra $I(T,\nu)$ by

$$I(T, \nu) = fd_\alpha(T) \cdot Id_\alpha(T, \nu) + fd_{rc}(T) \cdot Id_{rc}(T, \nu) + \\ f_\alpha(T) \cdot I_\alpha(T, \nu) + f_{rc}(T) \cdot I_{rc}(T, \nu) \tag{3}$$

where T is the temperature and ν is the Raman frequency. The terms $fd_\alpha(T)$ and $f_\alpha(T)$ are the fractional α-helix content of the deuterated and nondeuterated segments of AdP, and $fd_{rc}(T)$ and $f_{rc}(T)$ are the fraction random coil content of the deuterated and nondeuterated segments of AdP and are normalized by the total number of amide bonds in the peptide (deuterated plus non-deuterated). $Id_\alpha(T, \nu)$ and $Id_{rc}(T, \nu)$, are the spectra of the pure α-helix and the random coil (rc) conformations of the deuterated segments of AdP. $I_\alpha(T, \nu)$ and $I_{rc}(T, \nu)$ are the α-helix and random coil spectra of the nondeuterated peptide segments. Thus, $fd_\alpha(T) + fd_{rc}(T) + f_\alpha(T) + f_{rc}(T) = 1$.

The α-helical amide III frequency and band shape are temperature independent, while the AP random coil amide III shows modest temperature dependence.[1] Therefore, $Id_\alpha(T, \nu) = Id_\alpha(\nu)$ and $I_\alpha(T, \nu) = I_\alpha(\nu)$

We find that the random coil deuterated amide III band is also essentially temperature independent. This probably results

from the fact that C_α deuteration removes the variable contribution of C_α–H bending,[9–11] which is responsible for the large sensitivity of the amide III band to the peptide bond conformation.[9] Therefore, $Id_{rc}(T, \nu) = Id_{rc}(\nu)$ for the amide III spectral region (1200–1400 cm^{-1}).

Thus, we can modify eq 3

$$I(T, \nu) = fd_\alpha(T) \cdot Id_\alpha(\nu) + fd_{rc}(T) \cdot Id_{rc}(\nu) + f_\alpha(T) \cdot I_\alpha(\nu) + f_{rc}(T) \cdot I_{rc}(T, \nu) \quad (4)$$

At high temperature ($T \geq 70\ °C$), AP and AdP are essentially 100% random coil (Figure 2A and ref 1). Thus, n_d deuterated and n_n nondeuterated amide bonds ($n_d + n_n = n = 20$) occur in the random coil form. The high temperature, T_1, AdP spectrum $I(T_1,\nu)$ is thus, from eq 4

$$I(T_1, \nu) = \frac{n_d}{n} \cdot Id_{rc}(\nu) + \frac{n_n}{n} \cdot I_{rc}(T_1, \nu) \quad (5)$$

and the difference spectrum between high T_1 and low T_2 temperatures can be written

$$\Delta I = I(T_2, \nu) - I(T_1, \nu)$$
$$= fd_\alpha(T_2) \cdot [Id_\alpha(\nu) - Id_{rc}(\nu)] + f_\alpha(T_2) \cdot [I_\alpha(\nu) - I_{rc}(T_2, \nu)] - \frac{n_n}{n} \cdot [I_{rc}(T_2,) - I_{rc}(T_1, \nu)] \quad (6)$$

Here we used eq 4 for the low-temperature spectrum $I(T_2,\nu)$ and eq 5 for the high-temperature spectrum $I(T_1,\nu)$. Since the 1240 cm^{-1} AdP difference spectral peak results from the α-helix→random coil transition of the nondeuterated part of AdP, from eq 6 we obtain

$$\Delta I(\nu_1) = f_\alpha(T_2) \cdot [I_\alpha(\nu_1) - I_{rc}(T_2,_1)] - \frac{n_n}{n} \cdot [I_{rc}(T_2, \nu_1) - I_{rc}(T_1, \nu_1)] \quad (7)$$

Here ν_1 is 1240 cm^{-1} and $[Id_\alpha(\nu_1) - Id_{rc}(\nu_1)] = 0$, since there is no contribution of the deuterated segment to the 1240 cm^{-1} spectral change. Using the previously calculated[1] temperature-dependent AP UVRR spectra for the α-helix $I_\alpha(\nu)$ and random coil conformations $I_{rc}(T, \nu)$, we determined the temperature dependence of the α-helical fraction of the nondeuterated (internal) α-helical segments $f_\alpha(T_2)$ from eq 7. The temperature dependence of this calculated α-helical fraction is shown in Figure 2B, $\diamond$.

We calculated the α-helical fraction of the deuterated part of AdP from the UVRR spectra using the dependence of the 1325 cm^{-1} band Raman cross sections on the α-helix and random coil composition. Using values of $f_\alpha(T_2)$, obtained from eq 7 by using the 1240 cm^{-1} nondeuterated amide III band, we can calculate the product $fd_\alpha(T_2) \cdot [Id_\alpha(\nu) - Id_{rc}(\nu)]$ from eq 6 since all other parameters are known.

$$fd_\alpha(T_2) \cdot [Id_\alpha(\nu_2) - Id_{rc}(\nu_2)] = \Delta I(\nu_2) - f_\alpha(T_2) \cdot [I_\alpha(\nu_2) - I_{rc}(T_2, \nu_2)] + \frac{n_n}{n} \cdot [I_{rc}(T_2, \nu_2) - I_{rc}(T_1, \nu_2)] \quad (8)$$

where ν_2 is 1325 cm^{-1}. We obtained the value of $[Id_\alpha(\nu_2) - Id_{rc}(\nu_2)]$, which we assume is temperature independent,[12] from the measured value of $fd_\alpha(T)$ at $T = 0\ °C$ obtained by subtracting the α-helical fraction of the nondeuterated part of AdP from the calculated α-helical fraction of AP, since AP and AdP show identical α-helical fraction temperature dependencies, Figure 2A. These calculated values are shown by the ◆ in the Figure 2B. In the future we will directly determine more accurate values of $[Id_\alpha(\nu_2) - Id_{rc}(\nu_2)]$ and its actual temperature dependence from UVRR spectra of fully deuterated peptides.

References and Notes

(1) Lednev, I. K.; Karnoup, A. S.; Sparrow, M. C.; Asher, S. A. *J. Am. Chem. Soc.* **1999**, *121*, 8074–8086.

(2) Karplus, M.; Weaver, D. L. *Protein Sci.* **1994**, *3*, 650–668.

(3) Kim, P. S.; Baldwin, R. L. *Annu. Rev. Biochem.* **1990**, *59*, 631–660.

(4) Williams, K.; Causegrove, T. P.; Gilmanshin, R.; Fang, K. S.; Callender, R. H.; Woodruff, W. H.; Dyer, R. B. *Biochemistry* **1996**, *35*, 691–697.

(5) Poland, D.; Sheraga, H. A. *Theory of Helix-Coil Transition in Biopolymers*; Academic press: New York and London, 1970.

(6) Thompson, P. A.; Eaton, W. A.; Hofrichter, J. *Biochemistry* **1997**, *36*, 9200–9210.

(7) Thompson, P. A.; Munoz, V.; Jas, G. S.; Henry, E. R.; Eaton, W. A.; Hofrichter, J *J. Phys. Chem. B* **2000**, *104*, 378–389.

(8) Lednev, I. K.; Karnoup, A. S.; Sparrow, M. C.; Asher, S. A. *J. Am. Chem. Soc.* **2001**, *123*, 2388–2393.

(9) Asher, S. A.; Ianoul, A.; Mix, G.; Boyden, M.; Karnoup, A.; Diem, M.; Schweitzer-Stenner, R. *J. Am. Chem. Soc.* **2001**, *123*, 11775–11781.

(10) Overman, S. A.; Thomas, G. J., Jr. *Biochemistry* **1998**, *37*, 5654–5665.

(11) Oboodi, M. R.; Alva, C.; Diem, M. *J. Phys. Chem.* **1984**, *88*, 501–505.

(12) The random coil amide band Raman band frequencies and intensities show a significant temperature dependence,[1] presumably due to population of higher energy landscape ψ and φ Ramachandran angles. Much of the dependence of the random coil amide III band on the ψ angle results from a ψ dependent coupling with amide C_α–H bending motion.[9] This coupling cannot occur for the C_α deuterated derivative. Thus, the amide III band shows a negligible ψ angle conformational dependence and a much smaller temperature dependence.

(13) Chen, X. G.; Asher, S. A.; Schweitzer-Stenner, R.; Mirkin, N. G.; Krimm, S. *J. Am. Chem. Soc.* **1995**, *117*, 2884–2895.

(14) Ozdemir, A.; Lednev, I. K.; Asher, S. A. *Biochemistry* **2002**, *41*, 1893–1896.

(15) Shalongo, W.; Dugad, L.; Stellwagen, E. *J. Am. Chem. Soc.* **1994**, *116*, 2500–2507.